Author Manuscript

Author Manuscript

Author Manuscript

Author Manuscript

HHS Public Access

Author manuscript

Nanomedicine. Author manuscript; available in PMC 2022 May 24.

Published in final edited form as:

Nanomedicine. 2022 February ; 40: 102476. doi:10.1016/j.nano.2021.102476.

Optical biosensing of markers of mucosal inflammation

Obdulia Covarrubias-Zambrano, Ph.D.[a], **Massoud Motamedi, Ph.D.**[b], **Bill T. Ameredes, M.S., Ph.D.**[c], **Bing Tian, Ph.D.**[c], **William J. Calhoun, MD**[c], **Yingxin Zhao, Ph.D.**[c], **Allan R. Brasier, MD**[d], **Madumali Kalubowilage, Ph.D.**[a], **Aruni P. Malalasekera, Ph.D.**[f], **Asanka S. Yapa, Ph.D.**[a], **Hongwang Wang, Ph.D.**[a], **Christopher T. Culbertson, Ph.D.**[a], **Deryl L. Troyer, Ph.D., DVM**[e], **Stefan H. Bossmann, Ph.D.**[a,g,*]

[a]Department of Chemistry, Kansas State University, Manhattan, KS, USA

[b]Center for Biomedical Engineering, University of Texas Medical Branch, Galveston, TX, USA

[c]Institute for Translational Sciences and Department of Internal Medicine, University of Texas Medical Branch, Galveston, TX

[d]Institute for Clinical and Translational Research, University of Wisconsin-Madison, School of Medicine and Public Health, Madison, WI

[e]Department of Anatomy & Physiology, Kansas State University, Manhattan, KS, USA

[f]Department of Chemistry, Southwestern College, 100 College Street, Winfield, KS, USA

[g]The University of Kansas Medical Center, Department of Cancer Biology and The University of Kansas Cancer Center, Kansas City, KS, USA

Abstract

We report the design and adaptation of iron/iron oxide nanoparticle-based optical nanobiosensors for enzymes or cytokine/chemokines that are established biomarkers of lung diseases. These biomarkers comprise ADAM33, granzyme B, MMP-8, neutrophil elastase, arginase, chemokine (C-C motif) ligand 20 and interleukin-6. The synthesis of nanobiosensors for these seven biomarkers, their calibration with commercially available enzymes and cytokines/chemokines, as well as their validation using bronchoalveolar lavage (BAL) obtained from a mouse model of TLR3-mediated inflammation are discussed here. Exhaled Breath Condensate (EBC) is a

*Corresponding author at: The University of Kansas Medical Center, Department of Cancer Biology, Kansas City, KS, USA. sbossmann@kumc.edu (S.H. Bossmann).

The authors declare no competing financial interest.

Credit Author Statement

Obdulia Covarrubias-Zambrano, Madumali Kalubowilage and Aruni P. Malalasekera have performed the series of plate-reader experiments with biospecimens from the University of Texas, Medical Branch at Galveston.

Obdulia Covarrubias-Zambrano, Bill Ameredes and Christopher T. Culbertson have performed the statistical analyses.

Asanka S. Yapa, Madumali Kalubowilage and Hongwang Wang have synthesized all components of the nanobiosensors, which were assembled by Madumali Kalubowilage, Hongwang Wang, and Obdulia Covarrubias-Zambrano.

Allan Brasier, Massoud Motamedi, William Calhoun and Bill Ameredes have planned the reported mouse and human studies and selected the biospecimens.

Bing Tian, Yingxin Zhao, and Allan R. Brasier have performed the mouse experiments.

Deryl L. Troyer and Stefan H. Bossmann have designed all nanobiosensor experiments and have written the final version of the manuscript, to which all co-authors have contributed.

Appendix A. Supplementary data

Supplementary data to this article can be found online at https://doi.org/10.1016/j.nano.2021.102476.

Author Manuscript Author Manuscript Author Manuscript Author Manuscript

minimally invasive approach for sampling airway fluid in the diagnosis and management of various lung diseases in humans (e.g., asthma, COPD and viral infections). We report the proof-of-concept of using human EBC in conjunction with nanobiosensors for diagnosis/monitoring airway inflammation. These findings suggest that, with nanosensor technology, human EBC can be utilized as a liquid biopsy to monitor inflammation/remodeling in lung disease.

Keywords

Nanomedicine; Nanodiagnostics; Iron/iron oxide core/shell nanoparticle; Optical biosensor; Lung inflammation

Sampling airway mucosal fluids: the need for a feasible liquid biopsy

There is considerable interest in sampling the airway fluid in the diagnosis and management of lung disease.[1,2] Liquid biopsies have the distinct advantage that no tissue samples have to be collected, minimizing patient discomfort and enabling repetitive studies over time to monitor disease progression.[3–5] However, for lung diseases, such as asthma, COPD (Chronic obstructive pulmonary disease) or lung cancer, the search for the best liquid biopsy is still in progress. Whereas blood-based liquid biopsies are rapidly becoming established in clinical diagnostics,[6] other methods for directly sampling airway biomarkers are desirable. Due to the unique physiology of the lung, disease-relevant biomarkers in the airways do not appear in the circulation, requiring distinct collection and measurement approaches.

Currently, airway sampling methods comprise bronchoalveolar lavage (BAL), bronchoscopic microprobes, induced sputum (IS), and exhaled breath condensates (EBCs). Briefly summarized in Table 1, these sampling techniques vary by: 1) level of invasiveness, 2) bias for sampling distinct regions of the lung, 3) amounts recovered, and 4) types of biomolecules sampled.[2] BAL is a highly invasive investigational tool that directly samples regions of the airway by dilution. Databases have been established that are cataloging the proteins obtained by BAL fluid extraction.[7,8] Similarly invasive, the bronchoscopic microprobe is an adsorptive tip capable of sampling fluid and cells locally in the airway.[9] IS is an alternative collection technique by inhalation of hypertonic saline that confers the added advantage of sampling the secretory products of the proximal and distal airways through normal mucus transport.[10] Both BAL and IS contaminate the specimen with sodium chloride, so measurements of electrolytes are precluded. All bronchoscopy-based methods also introduce lidocaine or other anesthetic agents into the recovered specimens. Finally, for study of microbiota, there is the potential to contaminate bronchoscopy-derived specimens with upper airway flora. With respect to patient comfort, it is of importance that all methods for obtaining liquid biopsies except EBC require some level of anesthesia (e.g., BAL or bronchoscopy), or unpleasant utilization of hypertonic saline (e.g., induction of sputum expectoration). In contrast, enhanced breath condensate (EBC) is a method of collection in which patients freely exhale with low effort into a cooled condensing collection device, requiring no anesthesia or induction, and little coaching. EBCs primarily sample epithelial-derived metabolic products and nanostructures of biological origin. They are enriched in water, water soluble gases, hydrogen peroxide, leukotrienes, isoprostanes,

Author Manuscript Author Manuscript Author Manuscript Author Manuscript

and small proteins, which can serve as biomarkers for lung diseases.[11] However, there are challenges with the potential for salivary protein contamination, low volume of collected material, dilution of the specimen by condensed water vapor, and limited protein sampling.[2] One potential strategy to circumvent these obstacles is the search for signature enzymes and chemokines/cytokines in EBC that can be detected in extremely small concentrations. Although this approach potentially limits the number of potential biomarkers that can be measured, it has the distinct advantage that point-of-care-devices can be designed without requiring collection of patients' blood, BAL, or sputum. (See Scheme 1.)

Optical nanobiosensors for the quantitative determination of proteases, enzymes capable of posttranslational modifications, and cytokines

Accordingly, since 2007, the Sensor Team at Kansas State University has been continuously improving their patented bionano-sensor technology for the ultra-sensitive detection of proteases,[14–16] and post-translational modifications,[17] in serum and milk.[18] This nanobiosensor technology is based on the optical properties of magnetic Fe/Fe_3O_4 core/shell nanoparticles that have been linked to fluorophores and FRET-quenchers and has been developed for invitro diagnostics.[19–23] One of the characteristics of this technology is that numerous proteases, as well as arginase, can be detected at sub-femtomolar activities.[19,20,23] Furthermore, enzymatic activity can be determined in a wide range (10^{-5} to 10^{-16} M).[19,20,22] Here, we report the expansion of our proven nanobiosensor technology to detect and establish reliable biomarkers for mucosal inflammation in EBC. For that purpose, we are introducing novel nanobiosensors for the detection of disintegrin and metalloproteinase domain 33 (ADAM 33),[24] granzyme B,[25] chemokine (C-C motif) ligand 20 (CCL20)[26] and interleukin-6 (IL-6),[27] as well as improved nanobiosensors for arginase,[28] which will be used for the detection of proteases and cytokines/chemokines in EBC, together with the established nanobiosensors for neutrophil elastase (NE) and matrix metalloproteinase-8 (MMP-8).[21,23]

Pro-inflammatory factors in lung disease

The basis for our interest in the pro-inflammatory factors mentioned above is their known involvement in inflammatory lung diseases. For example, ADAM 33 has been identified as key protease in airway hyper-responsiveness and airway wall remodeling.[24] Granzyme B is a serine protease that is delivered via perforin to target cells by cytotoxic lymphocytes, and it plays an important role in innate and adaptive immunity. Since the latter requires pro-inflammatory signaling, granzyme B is also involved in numerous inflammatory processes associated with several lung diseases.[25] CCL20 is a small cytokine (70 amino acids), belonging to the CC chemokine family, which attracts lymphocytes and dendritic cells as part of the inflammatory process, and is implicated in the formation and function of mucosal lymphoid tissues by binding to its receptor CCR6 (C-C Motif Chemokine Receptor 6).[26] IL-6 (183 amino acids) is a multifunctional pro-inflammatory cytokine and anti-inflammatory myokine.[27] It is a key player in lung disorders involving inflammation, remodeling and fibrosis.[29] In chronic airway diseases, such as asthma and COPD, elevated arginase activity reduces the availability of L-arginine, thus causing inflammation, airway contractility, and remodeling.[28] NE[30] and MMP-8[31] cleave extracellular matrix proteins, which results in the formation of matrikines (signaling oligopeptides capable

Author Manuscript Author Manuscript Author Manuscript Author Manuscript

of increasing the chemotaxis of neutrophils and other defensive cells), which are again pro-inflammatory.[31] In summary, this group of pro-inflammatory factors forms a solid basis for investigations utilizing nanobiosensors for their detection within liquid biopsy samples of small quantities originating from the lung.

Results and discussion

I. Nanobiosensors for protease detection

Fe/Fe_3O_4 nanoparticles were used for the assembly of nanobiosensors for protease detection described in this study. These nanoparticles have a well-defined core/shell structure, with an average diameter of 13 ± 0.5 nm for the Fe(0) core and 2.0 ± 0.5 nm for the Fe_3O_4 shell thickness, resulting in nanoparticles with an average size of 15 nm.[19] The HRTEM image reveals the polycrystalline nature of the nanoparticles and their distinctive core/shell structure. Dopamine forms robust organic coatings with binding constants of the order of 10^{15} L/mol,[32] and it also increases the water-solubility of the nanosensors from <0.1 g • L^{-1} to >5 g • L^{-1} [19]. Porphyrins have been used as cleavable fluorescent dyes because their photophysical properties are well-characterized.[33] Cyanine (Cy) 5.5 has been co-attached as FRET quencher due to its large molar extinction coefficient and suitable Förster radius.[34] Therefore, both dyes have been selected as a FRET pair for the nanobiosensors. The structure of the nanosensor composed of dopamine-coated Fe/Fe_3O_4, consensus sequence, TCPP (tetrakis-carboxyphenyl-porphyrin), and Cy 5.5 is shown in Figure 1. Importantly, Cy 5.5 is permanently linked to dopamine without using an enzyme-cleavable tether. Consequently, Cy 5.5 remains permanently bonded to the nanoparticle during the protease detection process. Based on mathematical modeling taking into account the surface of the Fe/Fe_3O_4 nanoparticle, the tether lengths and the Förster radii of TCPP and Cy 5.5, we have calculated that optimal quenching can be observed for 35 TCPP and 50 Cy 5.5 dyes at the nanoparticle's surface.[35,36] Due to additional plasmonic quenching by the Fe/Fe_3O_4 nanoparticles, the nanobiosensor shows only minimal fluorescence intensity.[19] Once the oligopeptide tether is cleaved by a protease with high selectivity for the selected consensus sequence, the fluorescence of TCPP increases significantly (ON mode) and can be utilized for measurements. This technology has been successfully utilized for the detection of early breast[20] and pancreatic[23] human cancers by means of liquid biopsies, using serum.

ADAM 33, granzyme B, Neutrophil elastase and MMP-8 have been selected as proteases of interest for exhaled breath-based liquid biopsies. Their consensus sequences are summarized in Table 2.[37] The synthesis of the nanobiosensors is described in the Experimental Section. (See Table 3.)

II. An improved nanobiosensor for arginase detection

Two isoforms of arginase, arginase I (L-arginase ureahydrolase) and arginase II, are found in mammals. Both arginases metabolize L-arginine to L-ornithine and urea according to the following equation[38]:

Besides their fundamental role in the hepatic urea cycle, arginases are key players in the immune system. It is noteworthy that arginases and nitric oxide (NO) synthases compete

Author Manuscript Author Manuscript Author Manuscript Author Manuscript

for the substrate L-arginine. Disrupted L-arginine homeostasis causes inflammation, airway contractility, and remodeling in lung tissue.[28]

Utilizing these properties, we designed the first nanobiosensor for the combined detection of arginases I and II activity, in 2017.[22] It featured the oligopeptide GRRRRRRRG (GR_7G) (g: Glycine, R: arginine) between a central, dopamine-covered Fe/Fe_3O_4 nanoparticle (see Figure 1, B) and a pair of energy transfer resonant fluorescein dyes (cyanines 5.5 and 7.0). Specificity for arginases vs. (inducible) NO-synthases, which both use L-arginine as substrate was achieved taking advantage of the biochemical characteristics of both groups of enzymes. Arginases are capable of converting arginine units within an (oligo) peptide to ornithine, whereas inducible NO-synthases can only convert the free amino acid L-arginine to L-citrulline.[39,40] The functional principle of this first fluorescence nanobiosensor for the detection of a posttranslational modification is that GO_7G (o: ornithine) possesses a distinctly different oligopeptide dynamic than GR_7G, which translates into detectable changes of nanoparticle-fluorophore interaction. It is noteworthy that the first generation of nanobiosensor for L-arginine detection had a sub-picomolar limit of detection (LOD) for arginase activity. Whereas this sensitivity appears to be suitable for studying arginase activities in tissue and serum, it is not sufficient for studying arginase activity in EBC. Therefore, we have redesigned the second generation of nanobiosensor for detection of low levels of arginase activity for this specific purpose.

Inspired by the success of the nanobiosensors for protease detection (Figure 1, A), we have exchanged the Cy 5.5 and 7.0 FRET pair against TCPP (donor) and Cy 5.5 (acceptor). This approach takes additional advantage of the ability of the guanidino side chain of arginase to undergo effective proton transfer quenching of photo-excited states.[41] Therefore, an increase in TCPP fluorescence is observed upon enzymatic conversion of GR_7G into GO_7G, which is caused by the conversion of arginine, which is a proton-quencher of TCPP, into ornithine, which is not a photo-quencher of TCPP.

III. Nanobiosensors for cytokine detection

The third class of nanobiosensors features supramolecular recognition sequences for cytokines or other biological targets. As shown in Figure 2, B, the distance between the central Fe/Fe_3O_4 nanoparticle and oligopeptide-tethered fluorescent dye (TCPP) increases upon cytokine binding by a supramolecular recognition sequence. The latter can bind to either a functional or non-functional epitope of the cytokine. Binding to non-functional epitopes has the advantage of not having to compete with cytokine receptors. However, it has to be confirmed by means of crystal structure determination, 3D-NMR studies, or molecular modeling that the epitope of interest is accessible and not concealed within the cytokine's 3D structure.

A typical procedure for finding and optimizing a supramolecular recognition sequence is described as follows. The primary and tertiary structures of the target (e.g. interleukin-6) are retrieved from a data bank (e.g. UniProt[43] or Protein Data Bank[44]). The tertiary structure of the target is then redefined using the software packages developed by the **Protein Structure Bioinformatics Group** of the Swiss Institute of Bioinformatics Center, University of Basel, Switzerland.[45] A docking procedure between the optimized target and the antibody's light

Author Manuscript Author Manuscript Author Manuscript Author Manuscript

or heavy chains is performed using the Mobyle platform developed by the Institut Pasteur Biology IT Center, Paris, France.[46] This procedure reveals the real epitopes on the target. A final "site finder" procedure is then performed on the Mobyle platform docking the epitope of the target to the optimized structure of the antibody (Ab) fragment. This structure reveals the peptide sequence of the Ab fragment that is actually responsible for binding to the target. If this sequence is linear, it will be synthesized and placed between Fe/Fe_3O_4 and TCPP. If it is not linear, or if the LOD of the resulting nanobiosensor is not at least 10^{-14} M, the *in-silico* procedure is repeated using the structural information from another MAB.

The calibrations of the nanobiosensors for detecting interleukin-6 (IL-6) and C-C motif chemokine 20 (CCL 20) indicate that both nanobiosensors are capable of measuring their respective cytokine over eight orders of magnitude. Furthermore, both reach femtomolar LOD's. The supramolecular binding sequence for recognizing IL-6 is GANRPAQAWMLG. For supramolecular CCL 20 detection, GTQWWVVCQQFG was employed.

Generally, the length of the tether has to be optimized to ensure optimal signal-to-noise, and a broad range of detection. In order to compete with the methods for cytokine detection discussed above and to be able to detect cytokines in biospecimens without prior enrichment, the LOD of this technology should be at least ten times more sensitive than ELISA.

It is important to note that this technology can easily be extended to other enzymes, cytokines, or toxins. In all cases where an epitope can be identified, an oligopeptide (peptide aptamer) can be designed *in-silico* that binds to the target with binding constants $K_B > 10^{15}$ M, permitting the ultra-sensitive fluorescence detection of this binding event. As our initial results demonstrate, this technology can reach sub-femtomolar LOD, and is therefore at least ten times more sensitive than the most sensitive immunoassays and related technologies, making it suitable for detection of targets within EBC fluid.

IV. Detection of arginase and matrix metalloproteinase activities and cytokines in mouse bronchoalveolar lavage (BAL)

The immunostimulant polyinosinic:polycytidylic acid (poly IC), a potent agonist of Toll-like Receptor (TLRE3), was chronically administered to eight mice to induce neutrophilic inflammation and injury-repair.[47] A second group of eight mice was treated with phosphate buffered saline (PBS, control). ADAM33, granzyme B, MMP-8, neutrophil elastase, arginase, CCL20 and interleukin-6 were analyzed in BAL using the nanobiosensor detection technology described above. All selected biomarkers, with the exception of CCL20, indicate that the mice receiving poly IC showed a clearly discernible inflammatory response, compared to the control group treated with PBS only. Box plots of the activities of the investigated enzymes and the concentrations of the cytokines/chemokines are shown in Figures 3–6.

The data shown in Figures 3–6 clearly indicate that statistically significant differences in the activity of signature enzymes and the concentration of cytokines/chemokines in mice treated with poly-IC vs. PBS can be observed in BAL. It should be noted that there are significant homologies between mice, since the protein-coding regions of the mouse

Author Manuscript Author Manuscript Author Manuscript Author Manuscript

and human genomes are 85% identical.[37] However, we cannot calculate exact enzymatic activities and chemokine/cytokine concentrations for the performed mouse experiments, because our validation and calibration experiments were carried out with recombinant human proteins (see below). BAL is principally suited for liquid biopsies utilizing the nanobiosensor technology. However, as discussed above, the collection of BAL from human patients is problematic due to the requirement of anesthesia. Therefore, we have expanded this study by including exhaled breath condensate from a total of six patients. We are aware that these results are only preliminary. However, they permit the evaluation of the suitability of EBC for Liquid Biopsies.

V. Measurements of protease activities and cytokine/chemokine concentrations in exhaled breath condensate

In Figure 7 and Table 4, the activities of four protease biomarkers for pulmonary dysfunction, ADAM 33,[24] granzyme B,[25] matrix-metalloproteinase-8[31] and neutrophil elastase,[30] a cytokine (interleukin-6)[27] and C-C motif chemokine 20,[26] as well as arginase[26], are shown. These results clearly indicate that measurements of the activity of signature proteases of lung diseases are possible using EBC for liquid biopsies. Because of the lack of other measurements in EBC, conclusive comparisons with the results of other research endeavors cannot (yet) be drawn. While the sample number was small (three non-asthmatic healthy human subjects and three patients diagnosed with mild asthma), clear numerical trends were visibly discerned, and a *t* test with equal variance indicated significant differences in EBC biomarker levels that were associated with the diagnosis of asthma. Whereas the healthy human subjects did not show any measurable activity for ADAM 33, granzyme B and neutrophil elastase ($< 10^{-16}$ mol per liter), all three biomarkers were clearly detectable in the group of asthmatic persons. Enzymatic activities were ranging from 2.6×10^{-15} to 2.0×10^{-12} mol L^{-1} for ADAM 33, from 4.6×10^{-14} to 4.0×10^{-12} mol L^{-1} for granzyme B and from 9.0×10^{-16} to 6.2×10^{-14} mol L^{-1} for neutrophil elastase. It is noteworthy that the MMP-8 activities for healthy volunteers ranged from 2.8×10^{-13} to 7.6×10^{-11} mol L^{-1}, whereas significantly lower activities were obtained for the group of asthma patients (2.6×10^{-16} to 1.2×10^{-14} mol L^{-1}). The number of investigated human subjects in this study too small to formulate a conclusive general paradigm here, but our results indicated that future studies should likely revisit MMP-8 and several other biomarkers in healthy vs. asthmatic human subjects.

The detection of the chemokine CCL20[26] and the cytokine interleukin-6[27] has been achieved, to the best of our knowledge, for the first time employing a Fe/Fe_3O_4 core/shell nanoparticle-based nanobiosensor. Collecting EBC proved to be a viable method for liquid biopsies for cytokine/chemokine detection in patients with lung disease. The detectable concentration ranges in healthy volunteers and asthma patients were 2.8×10^{-14}–2.4×10^{-12} mol L^{-1} and 8.0×10^{-12}–1.3×10^{-11} mol L^{-1}, respectively (Figure 8). Whereas interleukin-6 concentrations were not detectable in healthy volunteers, they ranged from 1.5×10^{-10} to 5.0×10^{-9} mol L^{-1} is asthma patients, indicating that interleukin-6 is an important biomarker for lung injury, as has been established before by using a tailored immunoassay.[48] These initial data points suggest that the Fe/Fe_3O_4 core/shell nanoparticle-

Author Manuscript Author Manuscript Author Manuscript Author Manuscript

based nanobiosensors should have the sensitivity to be useful in measuring chemokines and cytokines in EBC.

VI. Measurements of arginase activities in exhaled breath condensate

Arginase converts L-arginine into L-ornithine, which is further metabolized to L-proline, L-hydroxyproline, and then collagen, potentially leading to fibrosis.[28,49] As shown in Figure 8 and Table 4, arginase activity could be detected in EBC of the healthy control group (3.6×10^{-15}–5.0×10^{-15} mol L^{-1}) and the group of mild asthma patients (1.2×10^{-12}–6.0×10^{-12} mol L^{-1}). Note that the average arginase activity increased by three orders of magnitude in asthma patients, compared to healthy human subjects.

Conclusions

Exhaled breath condensate (EBC) is a minimally invasive liquid biopsy approach that directly samples airway epithelial-derived metabolic products. Here, we have extended the optical nanobiosensor technology that was originally developed for the quantification of cancer-related proteases in serum[3,19–23] for the measurement of biomarkers of lung diseases in murine BAL and human EBC samples. The data obtained clearly indicate that the nanobiosensor technology can be used to determine proteolytic activities and chemokine/cytokine concentrations. Apparent differences in enzymatic activities or cytokine/chemokine concentrations were detected for asthma patients vs. healthy volunteers for ADAM33, granzyme B, MMP-8, neutrophil elastase, arginase, chemokine (C-C motif) ligand 20 and interleukin-6. This initial study has indicated that nanobiosensors can be utilized to collect potentially useful data on factors associated with lung pathology from within BAL and EBC samples from patients with lung disease. It should be emphasized that EBC is much easier to obtain than BAL from human patients and enables serial measurements to monitor disease progression over time or in response to therapeutic interventions. Our results indicate that collection and measurement of Liquid Biopsies utilizing EBC from lung disease patients could possibly become a standardized approach, leading to an improved standard of care.

Experimental Section

Procedure for BAL collection from mice

Bronchoalveolar lavage fluid (BALF) was collected from C57Bl6 mice that were administered polyinosinic:polycytidylic acid (poly I:C), a viral RNA pattern mimic that induces TLR3-associated airway inflammation, as previously described.[50] These experiments were performed according to the NIH Guide for Care and Use of Experimental Animals and approved by the University of Texas Medical Branch (UTMB) Animal Care and Use Committee (approval no. 1312058A). Briefly, either PBS (50 μL) or poly I:C (Sigma-Aldrich, 500 μg/dose in 50 μL PBS) was administered intranasally every other day over a period of 30 days, followed by an inflammation resolution phase of 12 days, at which time the mice were humanely terminated and BALF was collected using small sequential aliquots of PBS (0.5 ml). After separation from BAL leukocytes, the resultant BALF supernatant was frozen at −80 °C for subsequent cytokine and biomarker measurements.

Author Manuscript Author Manuscript Author Manuscript Author Manuscript

Procedure for EBC collection and storage

EBC samples were collected from human subjects as previously described[51], using commercial R-tube equipment. Samples were frozen immediately at −80 °C until analyzed.

Statistical analysis

An *F* test was used to determine if data had equal or unequal variance. After determining the variance for each dataset, a *t* test with equal variance or a *t* test with unequal variance (Welch's *t* test) was used to perform the statistical analysis to compare both the mouse BAL data (PBS vs. PolyIC) and the human EBC data (healthy vs. mild asthma) groups, for each biomarker. The null hypothesis was rejected when the *P* value was ≤0.05, determining that a statistically significant difference was present between the groups being compared. In the case of the mouse BAL data, the differences were found to be highly significant at the $P < 0.01$ level, as reported within the mouse BAL figures. These significant differences were annotated on each bar graph by marking with asterisks.

Synthesis of nanobiosensors

Detailed descriptions of the syntheses of nanobiosensors and the required components (dopamine Fe/Fe_3O_4 nanoparticles, oligopeptides, TCPP, and cyanine 5.5) have been reported in our previous studies.[19,20,22,23] There, all required steps are discussed in detail. Briefly, the nanobiosensors that are utilized[21,23] and reported here for the first time (ADAM33, granzyme B, (improved) arginase, CCL20, IL-6) were assembled from dopamine coated Fe/Fe_3O_4 nanoparticles, cyanine 5.5, and peptide sequences that were linked to TCPP on resin.[19] In order to achieve this synthesis, a solution was prepared by completely dissolving 64 mg of TCPP linked peptide sequence, 37 mg of Cy 5.5, 45 mg of EDC and 45 mg of DMAP in 30 mL of anhydrous DMF. In a separate vial, 450 mg of dopamine coated Fe/Fe_3O_4 nanoparticles was dispersed in 10 mL of anhydrous DMF by sonicating for 20 min. Both solutions were then mixed, sonicated for 10 min, and incubated overnight in a shaker at room temperature. After overnight incubation, the resulting nanobiosensor was collected via centrifugation (5 min at 10,000 RPM), washed with DMF to removed excess dye and unbound components, follwed by five washes with cold ether (263 K). After each washing step, the nanobiosensor was collected via centrifugation. Nanobiosensor was then collected and dried with argon gas. The nanobiosensors can be stored for more than 1 year at 253 K under argon.

The calibration procedures and curves are shown in the SI section.

Supplementary Material

Refer to Web version on PubMed Central for supplementary material.

Funding sources

This work was funded by NSF (CBET 1804416 (SHB/MM/CK), 1826982 (SHB) and EFMA 2032751 (SHB/MM/BTA) and EFMA 2129617 (SHB/MM/CK); NIH (The NHLBI Severe Asthma Research Project (SARP) HL-69130 (WJC); The UTMB Clinical and Translational Science Award (CTSA) NIH/NCATS 8UL1TR000071 (ARB/WJC); PO1 AI068865 (ARB)); UTMB Sealy Center for Molecular Medicine (SCMM) (ARB/BT/YZ); The Brown

Author Manuscript Author Manuscript Author Manuscript Author Manuscript

Foundation (BTA); The University of Kansas Cancer Center (SHB); and Johnson Cancer Center at Kansas State (SHB).

Abbreviations:

ADAM 33	disintegrin and metalloproteinase domain
BAL	bronchoalveolar lavage
CCL20	chemokine (C-C motif) ligand 20
COPD	chronic obstructive pulmonary disease
EBC	exhaled breath condensate
FRET	Förster Resonance Energy Transfer
HEPES	(4-(2-hydroxyethyl)-1-piperazineethanesulfonic acid)
IL-6	interleukin-6
IS	induced sputum
MMP-8	matrix metalloproteinase-8
NE	neutrophil elastase

References

1. Brasier AR. Identification of innate immune response endotypes in asthma: implications for personalized medicine. Curr Allergy Asthma Rep 2013;13(5):462–8. [PubMed: 23793609]
2. Wiktorowicz JE, Jamaluddin M. Proteomic analysis of the asthmatic airway. Adv Exp Med Biol 2014;795:221–32. [PubMed: 24162912]
3. Bossmann SH, Liquid biopsies for early cancer detection. In Biomaterials for cancer therapeutics, 2nd edition, Evolution and innovation, Park g, Ed. Elsevier: Amsterdam, 2020; pp. 233–259.
4. Revelo AE, Martin A, Velasquez R, Kulandaisamy PC, Bustamante J, Keshishyan S, et al. Liquid biopsy for lung cancers: an update on recent developments. Ann Transl Med 2019;7(15) 349pp. [PubMed: 31516895]
5. Pisapia P, Malapelle U, Troncone G. Liquid biopsy and lung cancer. Acta Cytol 2019;63(6):489–96. [PubMed: 30566947]
6. Chen D, Xu T, Wang S, Chang H, Yu T, Zhu Y, Chen J. Liquid biopsy applications in the clinic. Mol Diagn Ther 2020;24(2):125–32. [PubMed: 31919754]
7. Noel-Georis I, Bernard A, Falmagne P, Wattiez R. Database of bronchoalveolar lavage fluid proteins. J Chromatogr B Analyt Technol Biomed Life Sci 2002;771(1–2):221–36.
8. Wattiez R, Falmagne P. Proteomics of bronchoalveolar lavage fluid. J Chromatogr B Analyt Technol Biomed Life Sci 2005;815(1–2):169–78.
9. Franciosi L, Govorukhina N, Ten Hacken N, Postma D, Bischoff R. Proteomics of epithelial lining fluid obtained by bronchoscopic microprobe sampling. Methods Mol Biol 2011;790:17–28. [PubMed: 21948403]
10. Kim J-S, Hackley GH, Okamoto K, Rubin BK. Sputum processing for evaluation of inflammatory mediators. Ped Pulmon 2001;32(2):152–8.
11. Horvath I, Hunt J, Barnes PJ, Alving K, Antczak A, Baraldi E, et al. Condensate, A. E. T. F. o. E. B., Exhaled breath condensate: methodological recommendations and unresolved questions. Eur Respir J 2005;26(3):523–48. [PubMed: 16135737]

Author Manuscript Author Manuscript Author Manuscript Author Manuscript

12. Ho T, Scallan C, Rezaee N, Hambly N, Cox PG, Kolb M, et al. Sputum quantitative cytometry in patients with interstitial lung disease and chronic cough. Respir Med 2020;170:106067. [PubMed: 32843182]
13. Economidou F, Samara KD, Antoniou KM, Siafakas NM. Induced sputum in interstitial lung diseases: novel insights in the diagnosis, evaluation and research. Respiration; international review of thoracic diseases 2009;77(3):351–8. [PubMed: 19092236]
14. Basel MT; Bosssmann SH; Troyer DL Protease assay. 8,969,027; 9,682,155; 9,731,034, 03/15/2015; 06/20/2017; 08/15/2017, 2015.
15. Basel MT; Bosssmann SH; Troyer DL Protease assay. 8,969,027; 9,682,155; 9,731,034, 02/28/2017, 2017.
16. Basel MT; Bosssmann SH; Troyer DL Protease assay. 8,969,027; 9,682,155; 9,731,034, 09/17/2014, 2017.
17. Bosssmann SH; Malalsekera AP; Troyer DL; Wang H; Wendel S; Zhu G Nanoplatforms for arginase, indoleamine 2,3-dioxygenase and tryptophan 2,3-dioxygenase detection by posttranslational modification. 10,376,599, 08/13/2019, 2019.
18. Bosssmann SH; Malalsekera AP; Samarakoon TN; Troyer DL; Wang H; Kalubowilage M Nanosensors for detecting enzymatic activity in dairy production. 10,416,144, 09/17/2019, 2019.
19. Wang H, Udukala DN, Samarakoon TN, Basel MT, Kalita M, Abayaweera G, et al. Nanoplatforms for highly sensitive fluorescence detection of cancer-related proteases. Photochem Photobiol Sci 2014;13(2):231–40. [PubMed: 24096539]
20. Udukala DN, Wang H, Wendel SO, Malalasekera AP, Samarakoon TN, Yapa AS, et al. Early breast cancer screening using iron/iron oxide-based nanoplatforms with sub-femtomolar limits of detection. Beilstein J Nanotechnol 2016;7:364–73. [PubMed: 27335730]
21. Voelz BE, Kalubowilage M, Bossmann SH, Troyer DL, Chebel RC, Mendonca LGD. Associations between activity of arginase or matrix metalloproteinase-8 (MMP-8) and metritis in periparturient dairy cattle. Theriogenology 2017;97:83–8. [PubMed: 28583613]
22. Malalasekera AP, Wang H, Samarakoon TN, Udukala DN, Yapa AS, Ortega R, et al. A nanobiosensor for the detection of arginase activity. Nanomedicine NBM 2017;13(2):383–90.
23. Kalubowilage M, Covarrubias-Zambrano O, Malalasekera AP, Wendel SO, Wang H, Yapa AS, et al. Early detection of pancreatic cancers in liquid biopsies by ultrasensitive fluorescence nanobiosensors. Nanomedicine (N Y, NY, U S) 2018;14(6):1823–32.
24. Holgate ST. ADAM metallopeptidase domain 33 (ADAM33): indentification and role in airways disease. Drug News Perspect 2010;23(6):381–7. [PubMed: 20697605]
25. Joeckel LT, Bird PI. Blessing or curse? Proteomics in granzyme research. Proteomics Clin Appl 2014;8(5–6):351–81. [PubMed: 24677694]
26. Ito T, Carson WFIV, Cavassani KA, Connett JM, Kunkel SL. CCR6 as a mediator of immunity in the lung and gut. Exp Cell Res 2011;317(5):613–9. [PubMed: 21376174]
27. Wolf J, Rose-John S, Garbers C. Interleukin-6 and its receptors: a highly regulated and dynamic system. Cytokine 2014;70(1):11–20. [PubMed: 24986424]
28. van den Berg MPM, Meurs H, Gosens R. Targeting arginase and nitric oxide metabolism in chronic airway diseases and their co-morbidities. Curr Opin Pharmacol 2018;40:126–33. [PubMed: 29729549]
29. Ran N, Pang Z, Gu Y, Pan H, Zuo X, Guan X, et al. An updated overview of metabolomic profile changes in chronic obstructive pulmonary disease. Metabolites 2019;9(6):111.
30. Sandhaus RA, Turino G. Neutrophil elastase-mediated lung disease. COPD 2013;10(Suppl 1):60–3. [PubMed: 23527919]
31. Wells JM, Gaggar A, Blalock JE. MMP generated matrikines. Matrix Biol 2015;44–46:122–9.
32. Xu C, Xu K, Gu H, Zheng R, Liu H, Zhang X, et al. Dopamine as a robust anchor to immobilize functional molecules on the iron oxide shell of magnetic nanoparticles. J Am Chem Soc 2004;126(32): 9938–9. [PubMed: 15303865]
33. Ishihara S, Labuta J, Van Rossom W, Ishikawa D, Minami K, Hill JP, et al. Porphyrin-based sensor nanoarchitectonics in diverse physical detection modes. Phys Chem Chem Phys 2014;16(21): 9713–46. [PubMed: 24562603]

Author Manuscript Author Manuscript Author Manuscript Author Manuscript

34. Sabanayagam CR, Eid JS, Meller A. Using fluorescence resonance energy transfer to measure distances along individual DNA molecules: corrections due to nonideal transfer. J Chem Phys 2005; 122(6)061103. [PubMed: 15740360]
35. Ben-Avraham D, Schulman LS, Bossmann SH, Turro C, Turro NJ. Luminescence quenching of ruthenium(II)-tris(phenanthroline) by cobalt (III)-tris(phenanthroline) bound to the surface of starburst dendrimers. J Phys Chem B 1998;102(26):5088–93.
36. Bossmann SH; Schulman LS In Luminescence quenching as a probe of particle distribution, Cambridge University Press: 1997; pp 443–459.
37. https://www.ebi.ac.uk/merops/. (accessed on 12/17/2020)
38. Munder M Arginase: an emerging key player in the mammalian immune system. Br J Pharmacol 2009;158(3):638–51. [PubMed: 19764983]
39. Di Costanzo L, Sabio G, Mora A, Rodriguez PC, Ochoa AC, Centeno F, et al. Crystal structure of human arginase I at 1.29-Å resolution and exploration of inhibition in the immune response. Proc Natl Acad Sci U S A 2005;102(37):13058–63. [PubMed: 16141327]
40. Li H, Raman CS, Glaser CB, Blasko E, Young TA, Parkinson JF, et al. Crystal structures of zinc-free and -bound heme domain of human inducible nitric-oxide synthase. Implications for dimer stability and comparison with endothelial nitric-oxide synthase. J Biol Chem 1999; 274(30):21276–84. [PubMed: 10409685]
41. Protein fluorescence. In: Lakowicz JR, editor. Principles of fluorescence spectroscopy. Boston, MA: Springer US; 2006. p. 529–75.
42. Gao PF, Li YF, Huang CZ. Plasmonics-attended NSET and PRET for analytical applications. TrAC, Trends Anal Chem 2020;124115805.
43. https://www.uniprot.org/. (accessed on 12/17/2020)
44. https://www.rcsb.org/. (accessed on 12/17/2020)
45. https://swissmodel.expasy.org/. (accessed on 12/17/2020)
46. https://mobyle.rpbs.univ-paris-diderot.fr/cgi-bin/portal.py#welcome. (accessed on 12/17/2020)
47. Tian B, Patrikeev I, Ochoa L, Vargas G, Belanger KAK, Litvinov J, et al. NF-κB mediates mesenchymal transition, remodeling, and pulmonary fibrosis in response to chronic inflammation by viral RNA patterns. Am J Respir Cell Mol Biol 2017;56(4):506–20. [PubMed: 27911568]
48. Bucchioni E, Kharitonov SA, Allegra L, Barnes PJ. High levels of interleukin-6 in the exhaled breath condensate of patients with COPD. Respir Med 2003;97(12):1299–302. [PubMed: 14682411]
49. Morris SM Jr. Recent advances in arginine metabolism: roles and regulation of the arginases. Br J Pharmacol 2009;157(6):922–30. [PubMed: 19508396]
50. Tian B, Liu Z, Litvinov J, Maroto R, Jamaluddin M, Rytting E, et al. Efficacy of novel highly specific bromodomain-containing protein 4 inhibitors in innate inflammation-driven airway remodeling. Am J Respir Cell Mol Biol 2019;60(1):68–83. [PubMed: 30153047]
51. Liu L, Teague WG, Erzurum S, Fitzpatrick A, Mantri S, Dweik RA, Bleecker ER, Meyers D, Busse WW, Calhoun WJ, Castro M, Chung KF, Curran-Everett D, Israel E, Jarjour WN, Moore W, Peters SP, Wenzel S, Hunt JF, Gaston B. Determinants of exhaled breath condensate pH in a large population with asthma National Heart, Lung, and Blood Institute Severe Asthma Research Program (SARP) Chest 2011;139(2):328–36, 10.1378/chest.10-0163 Epub 2010 Oct 21. [PubMed: 20966042]

Author Manuscript Author Manuscript Author Manuscript Author Manuscript

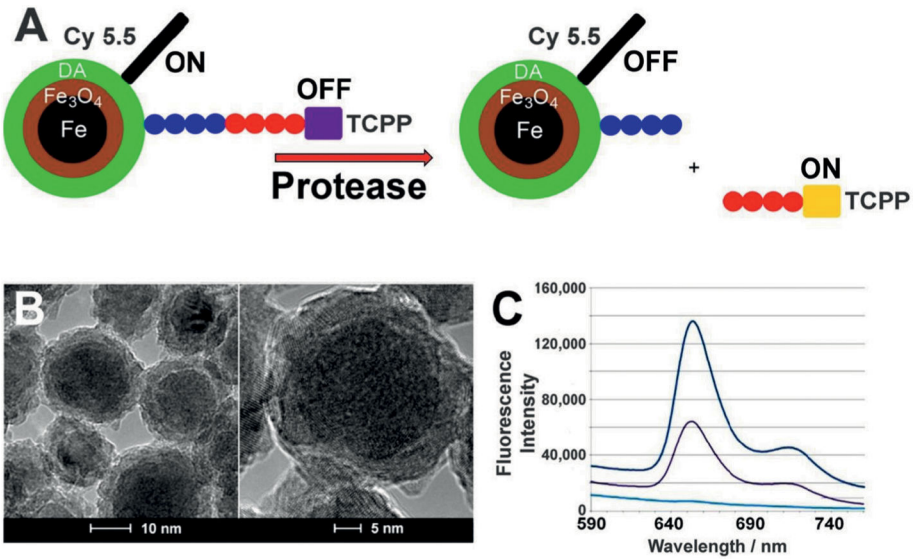

Figure 1.

(A) Design principles of a nanobiosensor for protease detection. The OFF mode (left side schematic) occurs when distance between fluorophore TCPP (tetrakis-carboxyphenyl-porphyrin), Fe/Fe_3O_4 nanoparticle, and FRET-acceptor cyanine (Cy) 5.5C is reduced; upon cleavage of the oligopeptide tether by a suitable protease present, this distance increases and leads to an increase in fluorescence intensity, which is called the ON mode (right side schematic). Blue and red colored circles indicate consensus sequences, as explained in Table 2. **(B)** TEM and HRTEM of dopamine-coated Fe/Fe_3O_4 core/shell nanoparticles showing basic core (darker areas) and shell (lighter areas) structure. **(C)** Typical emission spectra occurring from the nanosensor for MMP-13 after 1 h of incubation at 37 °C (λ_{exc} = 421 nm). Lower light blue line: buffer; middle black line: nanosensor; higher dark blue line: nanosensor after incubation with MMP-13.[19]

Author Manuscript Author Manuscript Author Manuscript Author Manuscript

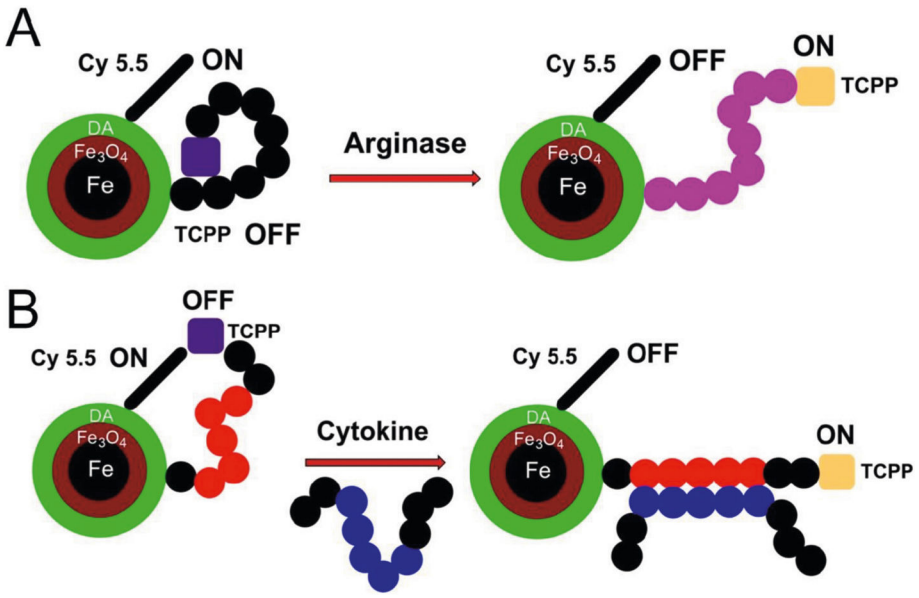

Figure 2.

(A) Design principles of the improved nanobiosensor for arginase detection. Due to the presence of seven L-arginine residues in G(R_7) TCPP is quenched by means of three quenching mechanisms: 1) plasmonic quenching, 2) FRET, and 3) proton transfer quenching. When L-arginase is modified by arginase (I + II) to L-ornithine, the dynamics of the tether changes, thus reducing plasmonic quenching and FRET. Due to the hydrolytic release of urea from L-arginine, proton transfer quenching is no longer possible, and the reaction ceases. The overall effect is switching on TCPP fluorescence, in response to arginase activity, which can then be quantified. **(B)** Design principles of nanobiosensors for cytokine/chemokine detection. Instead of a consensus sequence, the tether features a peptide-binding site for an epitope on the cytokine/chemokine of interest. Cytokine/chemokine binding triggers a conformational change of the tether, resulting in a statistical increase of TCPP and Fe/Fe_3O_4/Cyanine (Cy) 5.5, which decreases both plasmonic quenching and FRET. Consequently, fluorescence increase of TCPP is observed. Whereas the distance dependence of FRET processes decreases with r^{-6}, surface energy transfer, also known as plasmonic quenching,[42] drops off according to r^{-4} characteristics.

Author Manuscript Author Manuscript Author Manuscript Author Manuscript

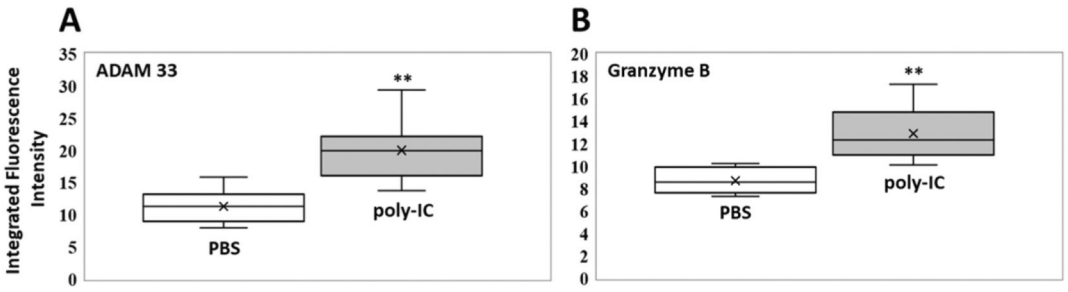

Figure 3.

Box plots (indicating the observed data range of integrated fluorescence intensity (BioTek Synergy H1) after 60 min of incubation at 300 K) for **(A)** ADAM 33 (left) and **(B)** Granzyme B (right) activities in mouse bronchoalveolar lavage for PBS (white; $n = 8$) vs. poly-IC in PBS (gray; $n = 8$). For both enzymes, ADAM 33 and Granzyme B, the differences in nanobiosensor fluorescence observed in the group of mice treated with poly-IC vs. the group treated with PBS were statistically significant (** $P < 0.01$). The LODs (0.1 femtomoles) for ADAM 33 and Granzyme B are 4.1 and 3.1 integrated fluorescence units, respectively.

Author Manuscript Author Manuscript Author Manuscript Author Manuscript

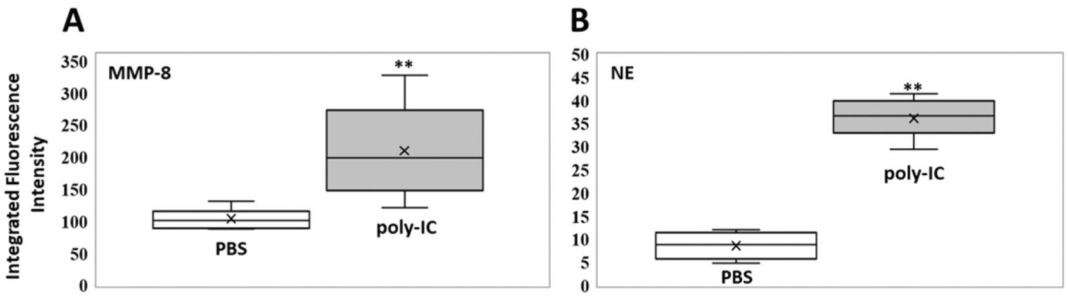

Figure 4.

Box plots (indicating the observed data range of integrated fluorescence intensity (BioTek Synergy H1) after 60 min of incubation at 300 K) for **(A)** MMP-8 (left) and **(B)** NE (right) activities in mouse bronchoalveolar lavage for PBS (white; $n = 8$) vs. poly-IC in PBS (gray; $n = 8$). For both enzymes, MMP-8 and NE, the differences in nanobiosensor fluorescence observed in the group of mice treated with poly-IC vs. the group treated with PBS were statistically significant (** $P < 0.01$). The LODs (0.1 femtomoles) for MMP-8 and NE are 7.3 and 5.2 integrated fluorescence units, respectively.

Author Manuscript Author Manuscript Author Manuscript Author Manuscript

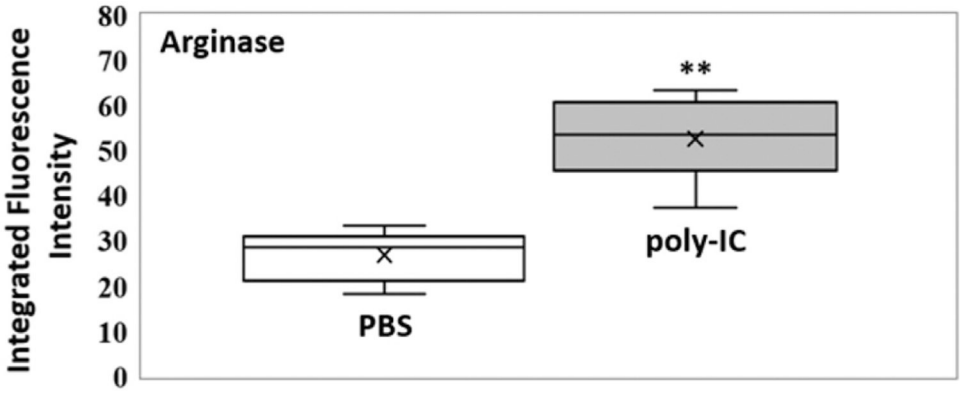

Figure 5.

Box plot (indicating the observed data range of integrated fluorescence intensity (BioTek Synergy H1) after 60 min of incubation at 300 K) for arginase activity in mouse bronchoalveolar lavage for PBS (white; $n = 8$) vs. poly-IC in PBS (gray; $n = 8$). For arginase the difference in nanobiosensor fluorescence observed in the group of mice treated with poly-IC vs. the group treated with PBS was statistically significant (**$P < 0.01$). The LODs (0.1 femtomoles) for arginase is 5.5 integrated fluorescence units.

Author Manuscript Author Manuscript Author Manuscript Author Manuscript

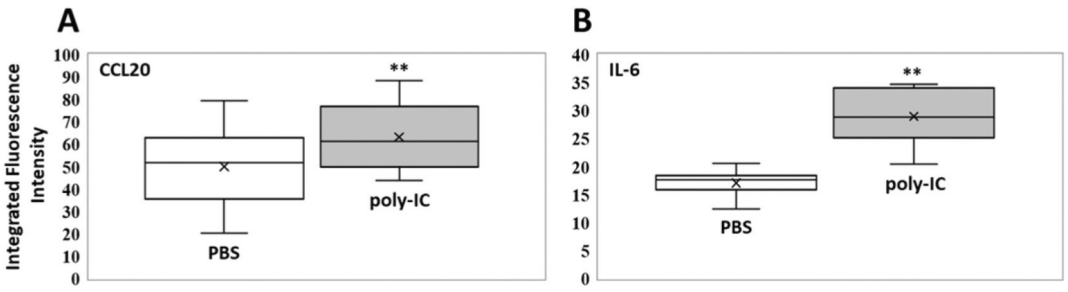

Figure 6.

Box plots (indicating the observed data range of integrated fluorescence intensity (BioTek Synergy H1) after 60 min of incubation at 300 K) for **(A)** CCL20 (left) and **(B)** IL-6 (right) concentrations in mouse bronchoalveolar lavage for PBS (white; $n = 8$) vs. poly-IC in PBS (gray; $n = 8$). For IL-6 the difference in nanobiosensor fluorescence observed in the group of mice treated with poly-IC vs. the group treated with PBS was statistically significant (** $P < 0.01$), whereas it was not significant (n.s.) for CCL20 ($P = 0.14$).The LODs (0.1 femtomoles) for CCL20 and IL-6 are 3.5 and 2.8 integrated fluorescence units, respectively.

Author Manuscript Author Manuscript Author Manuscript Author Manuscript

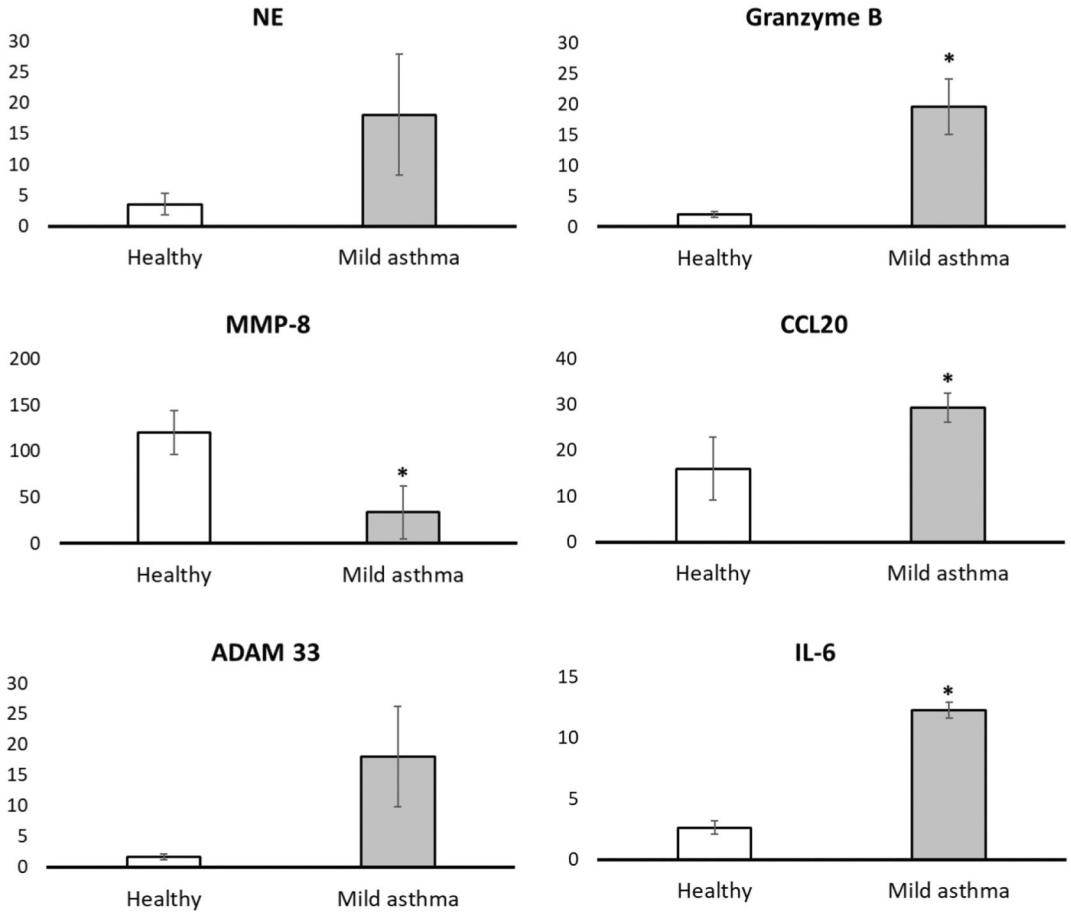

Figure 7.

Detection of the activity of four proteases (ADAM 33, Granzyme B, MMP-8, and neutrophil elastase) in exhaled breath condensate in three patients with mild asthma (no corticosteroids) vs. three patients without asthma as control group. The analytic procedure is described in detail in the Experimental Section. Significant differences ($P < 0.05$) are annotated on each bar graph by marking with an asterisk; all other comparisons between control (healthy) and mild asthma demonstrated numerically higher means but were not statistically significant.

Author Manuscript Author Manuscript Author Manuscript Author Manuscript

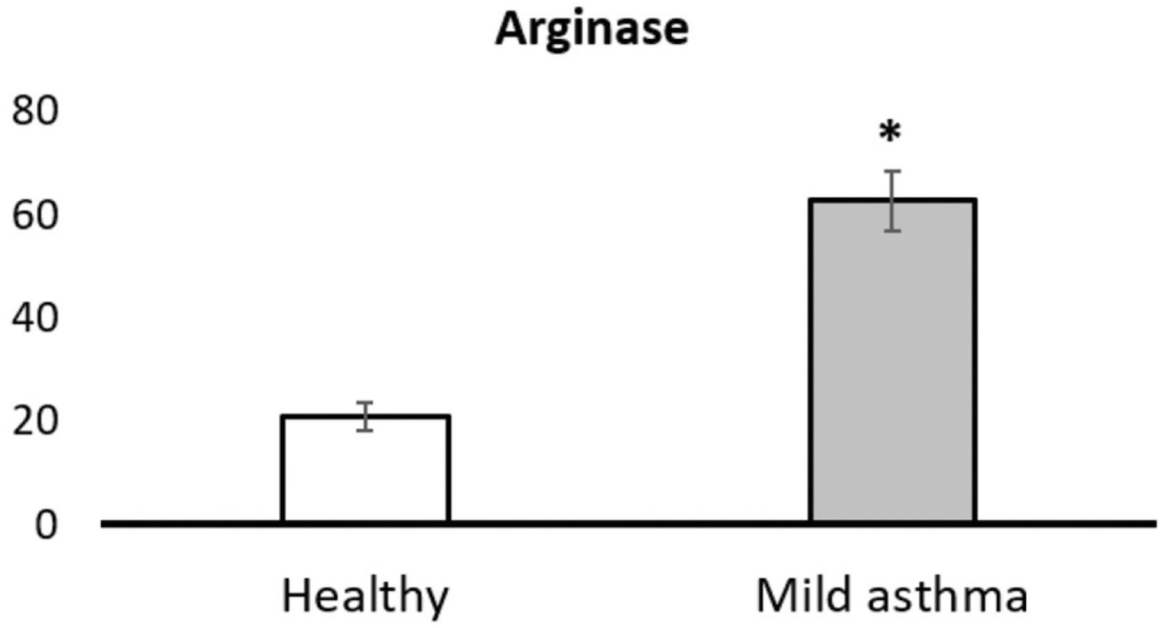

Figure 8.

Detection of the activity of arginase in exhaled breath condensate in three patients with mild asthma (no corticosteroids) vs. three patients without asthma as control group. The analytic procedure is described in detail in the Experimental Section. The differences in arginase activity between healthy and patient groups were found to be significant ($P < 0.05$).

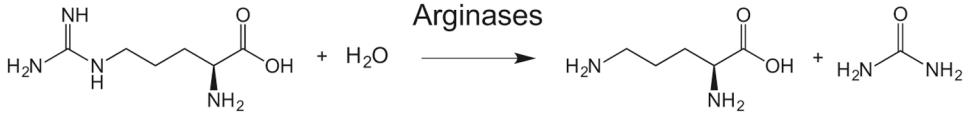

Scheme 1.

L-arginine is hydrolyzed by arginases I and II to L-ornithine and urea.

Author Manuscript Author Manuscript Author Manuscript Author Manuscript

Author Manuscript Author Manuscript Author Manuscript Author Manuscript

Table 1

Airway fluid sampling.

Typical approaches for sampling airway fluids.[1–13]

Approach	Volume recovered	Protein concentration and/or type	Limitations of approach
Bronchoalveolar lavage	50–100 ml	0.05–1.5 μg/pL Plasma proteins abundant in the presence of airway inflammation	Method is invasive; primarily for research application No consensus for recovery control or normalization
Induced sputum	0.5–3.0 ml of sputum + saline	Sample is mucous-rich, which may interfere with downstream analysis	Method samples proximal airway fluid; contamination with saliva can interfere with airway sampling
Nasopharyngeal aspirate	Protocol dependent	Mucous rich	Samples upper respiratory tract- regional
EBC	1 ml/5–15 min collection	No cells are obtained Cytokines IL-8, IL-1b, TNF, IL-10 detectable Gases and metabolites	Dilution controls needed Samples airway lining fluids and proteins, no cells recovered
Plasma	10–100 ml	Wide dynamic range in the milligram per milliliter range, requires depletion approaches	Not fully representative of airway proteins Large dynamic range of proteins complicates analysis

Author Manuscript

Author Manuscript

Author Manuscript

Author Manuscript

Table 2

Consensus sequences of proteolytic enzymes for clinical BAL and EBC analyses.

Enzyme	Consensus sequence	Reference
ADAM 33	GAGSQH-IRAEAG	this work
Granzyme B	GAGVEPN-SLEEAG	this work
Neutrophil elastase	GAGGEPV-SGLPAG	21
MMP-8	GAGPSG-LRGAG	23

Cleavable consensus sequences are shown in blue and red, and peptide sequences used as spacers (G, GA, GAG, AG) in nanobiosensors are in black. The consensus cleavage sites are marked with hyphens.

Author Manuscript

Author Manuscript

Author Manuscript

Author Manuscript

Table 3

Consensus sequences of proteolytic enzymes for clinical BAL and EBC analyses.

Enzyme	Consensus sequence	Reference
Arginase I + II	GRRRRRRR	22
C-C motif chemokine 20 (CCL20)	GTQWWVVCQQFG	This work
Interleukin-6	GANRPAQAWMLG	This work

Author Manuscript Author Manuscript Author Manuscript Author Manuscript

Table 4

Activities/concentrations of biomarkers for lung disease.

Biomarker	Activity/concentration Apparently healthy human subjects [mol L^{-1}]	Activity/concentration Mild asthma patients [mol L^{-1}]
ADAM 33	$< 10^{-16}$	2.6×10^{-15}–2.0×10^{-12}
Arginase	3.6×10^{-15}–5.0×10^{-15}	1.2×10^{-12}–6.0×10^{-12}
CCL20	2.8×10^{-14}–2.4×10^{-12}	8.0×10^{-12}–1.3×10^{-11}
Granzyme B	$< 10^{-16}$	4.6×10^{-14}–4.0×10^{-12}
Interleukin-6	$< 10^{-15}$	1.5×10^{-10}–5.0×10^{-9}
Matrix-metalloproteinase-8	2.8×10^{-13}–7.6×10^{-11}	2.6×10^{-16}–1.2×10^{-14}
Neutrophil elastase	$< 10^{-16}$	9.0×10^{-16}–6.2×10^{-14}